NUMERICAL COMPUTATIONS OF TURBOMACHINERY CASCADE TURBULENT FLOWS WITH SHOCKS BY USING MULTIGRID SCHEME *

Chen Naixing Zheng Xiaoqing Xu Yanji

The Institute of Engineering Thermophysics

Chinese Academy of Science

P.O. Box 2706, Beijing 100080

China

Abstract

A time–marching explicit finite volume method with multigrid scheme is presented for solution of steady, two–dimensional, transonic flows in turbomachinery cascades. The techniques for both Euler and Navier–Stokes solvers are the same. A new method for discretization of viscous terms is suggested. A body–fitted coordinate system is generated by a simple grid generation technique based on the staffs–springs system analogy method. Numerical solution results for two turbomachinery cascades are presented and compared with experimental data to demonstrate the accuracy, shock capturing capability and computational efficiency of the present method.

Introduction

The flows past through turbomachinery are very complex. In most instances, they are imcompressible or compressible, three–dimensional unsteady viscous and frequently separated flows. The flows may be subsonic, transonic or supersonic, with or without rotation, curvature, heat transfer, phase–changes, leakage and shock–boundary layer interaction. Because the progress has been made during the past decade in the area of computer science, numerical computational techniques, turbulence modeling, grid generation technique etc. The numerical computations provide an efficient tool for turbomachinery design and analysis. There are various numerical techniques used for numerical aerodynamics solution of turbomachinery flows. In these techniques time–marching methods [1–13], which may be either implicit or explicit, are widely used in external and internal flows. In the present paper are presented only the numerical computations by using the explicit finite volume time–marching method with multigrid scheme. In this paper the techniques for the solution of the Euler and the Navier–stoker equations are the same. They are discretized by finite volume approximation. The discretized algebraic equations are solved by Runge–Kutta techniqe [6] . The multigrid scheme [9] is also used in the present method for accelerating iteration convergence procedure. The various terms of the full Navier–Stokes equations are expressed and discretized by a more efficient method compared with previous ones. In this paper a grid generation technique is utilized for obtaining a body–fitted coordinate system. It is a special method based on the concept similar to that used for constitution of self–adaptive coordinate system. Calculations for both turbine and compressor cascades are carried out and compared with experiments.

Governing Equations and Boundary Conditions

The governing equations can be found in most references and text books. In the present paper the two–dimensional Reynolds–averaged Navier–Stokes equations, neglecting body force and heat sources, are written in finite volume formulation as:

$$\int_V \frac{\partial \rho}{\partial t} dV + \oint_S \rho(\vec{W} \cdot \vec{ds}) = 0$$

$$\int_V \frac{\partial(\rho \vec{W})}{\partial t} dV + \oint_S \rho \vec{W}(\vec{W} \cdot \vec{ds}) = \oint_S \vec{\tau}\, ds \qquad (1)$$

* Project supported by the National Natural Science Fundation of China

$$\int_v \frac{\partial e}{\partial t} dV + \oint_s e(\vec{W} \cdot \vec{ds}) = \oint_s (\vec{\tau} \cdot \vec{W}) ds + \oint_s C \left[\frac{\partial (p/\rho)}{\partial n}\right] ds$$

$$p = (k-1)(e - \frac{1}{2}\rho W^2) \tag{2}$$

where: V denotes a fixed volume with boundary S, $\vec{W}$ represents volocity vector, ρ, p, e represent density, pressure and total energy per unit volume, respectively. k is ratio of specific heats. $\vec{\tau}$ is the viscous stress acted on the surface with outer normal $\vec{n}$.

$$C = \frac{k}{k-1}\left(\frac{\mu_l}{P_{rl}} + \frac{\mu_t}{P_{rt}}\right) \tag{3}$$

P_{rl} and P_{rt} denote laminar and turbulent Prandtl numbers, respectively. μ_l and μ_t denote molecular and turbulent dynamic viscosities, respectively. Molecular viscosity, μ_l, is determined by Sutherland's law. Turbulent viscosity is estimated by turbulence model.

In solution of governing equations specification and enforcement of proper boundary conditions are essential to accurately capture the physics phynomena of the flow in turbomachinery. The unknown variables to be solved are velocity components, pressure, density, temperature or total energy per unit volume, etc. If there is no injection, a noslip boundary condition is imposed on velocity for the Navier–Stokes equations on the solid walls. For inviscid fluid flow, i.e. for solution of Euler equation, the velocity vectors are parallel to the blalde walls. The pressure at the wall can be obtained by assumption of zero normal gradient to the surface or by solution of the normal momentum equation. For temperature, either the blade surface temperature or the normal temperature gradient is given. For the heat transfer condition the temperature at blade surface is derived by heat transfer analysis of blade. For adiabatic wall of the present paper the normal temperature gradient is set to be zero.

The prescription of the conditions at inlet and exit boundaries far enough from the blade row depends on the flow regime, subsonic or supesonic. Here the total temperature and pressure and either the velocity components or the flow angles are given at inlet in the subsonic inlet case. The exit pressure is prescribed for cascade flow and its distribution is assumed to be uniform. The other flow variables are extrapolated from the interion point grid. For upstream and downstream regions enforcement of periodic boundary conditions is used.

Turbulence Model

Turbulence model is one of the essential ingredients for and accurate computation of turbomachinery flows. For turbulent flow the independent variables, excluding velocity components and thermodynamics parameters, in the equations are $\rho\overline{W_i' W_j'}$, $\rho\overline{W_i' e'}$. They are five additional variables have to be evaluated for two–dimensional flow. The most general transport equations for turbulence are the Reynolds stress equations. Many of the terms in these equations have to be modeled. Although the algebraic eddy–viscosity model, as indicated by many authors, is strictly valid only for two–dimensional flows with a mild pressure gradient, but for simplicity in the present paper is still used the Baldwin–Lomax [14] algebraic eddy viscosity turbulence model.

Expressions of Viscous Terms

Though the solution techniques for both N.S. and Euler equations are the same, but the main difference of expences between the numerical solutions of these two equations is essetial to estimate the viscous terms included in the Navier–Stokes equations. For improving solution efficiency a new method to discretize the viscous terms is proposed. It will be explained below.

The shear stress on the surface can be decomposed into two directions, i.e. normal and tangential, as follows:

$$\tau_n = -p + 2\mu\frac{\partial W_n}{\partial n} - \frac{2}{3}\mu div \vec{W}$$

$$\tau_\xi = \mu\left(\frac{\partial W_n}{\partial \xi} + \frac{\partial W_\xi}{\partial n}\right) \tag{4}$$

where W_n, W_ξ are the velocity components in normal, n, and tangential, ξ, directions, respectively.

By setting a new pressure parameter $\hat{p}$ to be the sum of $p + \frac{2}{3}\mu div \vec{W}$ and treating it as a separate term similar to the pressure in computation.

Then, the remainder of shear stress is

$$\vec{\tau} = \mu\frac{\partial \vec{W}}{\partial n} + \mu grad W_n \tag{5}$$

From the Cartesian coordinate system, x, y, adopted here, i.e.

$$W_n = \vec{W} \cdot \vec{n} = n_x W_x + n_y W_y \tag{6}$$

and

$$\frac{\partial \vec{W}}{\partial n} = \vec{u}_x \frac{\partial W_x}{\partial n} + \vec{u}_y \frac{\partial W_y}{\partial n}, \tag{7}$$

we have the formulas for expressing the gradient of normal velocity component, grad W_n, and the first derivative of velocity vector on normal direction, $\partial \vec{W} / \partial n$:

$$grad W_n = n_x grad W_x + n_y grad W_y \tag{8}$$

$$\frac{\partial \vec{W}}{\partial n} = \vec{u}_x(\vec{n} \cdot grad W_x) + \vec{u}_y(\vec{n} \cdot grad W_y) \tag{9}$$

Then, the remainder of shear stress can be rewritten as:

$$\vec{\tau} = \mu\left[n_x grad W_x + n_y grad W_y + \vec{u}_x(\vec{n} \cdot grad W_x)\right.$$

$$+\vec{u}_y(\vec{n}\circ gradW_y) \tag{10}$$

According to the difinition of gradient of a scalar, f,

$$gradf\approx\frac{1}{V}\sum_{l=1}^{n}f_l\Delta\vec{S}_l \tag{11}$$

where l is order of surface of a control volume, V, n is number of surfaces, in general speaking, $n$equals four for two–dimensional and six for three–dimensional flow problems, respectively. Applying Eq.(11) to the velocity components,

$$gradW_x=\frac{1}{V}\sum_{l=1}^{4}0+\left[\vec{u}_x(W_x\Delta S_x)_l+\vec{u}_y(W_x\Delta S_y)_l\right] \tag{12}$$

and denoting

$$G_i^j=\frac{1}{V}\sum_{l=1}^{4}(W_i\Delta S_j)_l \tag{13}$$

and i,j= 1,2 = x,y,
we have:

$$gradW_i=\sum_{j=1}^{2}G_i^j\vec{u}_j \tag{14}$$

Finally, the shear stress remainder can be expressed by the following expression:

$$\begin{aligned}\vec{\tau}&=\mu\frac{\partial\vec{W}}{\partial n}+\mu gradW_n\\&=\sum_{i=1}^{2}\tau_i\vec{u}_i\\&=\mu\sum_{i=1}^{2}\left(\sum_{j=1}^{2}n_jG_{ij}\right)\vec{u}_i\end{aligned} \tag{15}$$

where:

$$G_{ij}=\frac{1}{V}\sum_{l=1}^{4}(W_i\Delta S_j+W_j\Delta S_i)_l \tag{16}$$

From the above–mentioned derivation procedure it is obviously seem that only the following three G–parameters, G_{11},G_{12},G_{22}, for two–dimensional problem, are necessary to be estimate and stored for each control volume.

Now we are coming back to the pressure perameter, $\hat{p}$. According to the definition of divergence of velocity vector, $\vec{W}$, we have:

$$\begin{aligned}div\vec{W}&=\lim_{V\to0}\frac{\oint_S\vec{n}\circ\vec{W}ds}{V}\\&=\frac{1}{V}\sum_{l=1}^{4}\left[(W_x\Delta S_x)_l+(W_y\Delta S_y)_l\right]\\&=\frac{1}{V}\sum_{i=1}^{2}G_{ii}\end{aligned} \tag{17}$$

Then, the pressure parameter can be obtained as:

$$\hat{p}=p+\frac{\mu}{V}\sum_{i=1}^{2}G_{ii} \tag{18}$$

It is enable to summalize up that the computation of shear stress is mainly only the calculation of the G–parameters.

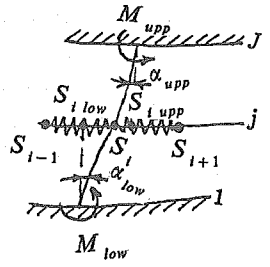

Fig.2. Principle scheme of ASSS method

Grid Generation Technique

In general speaking, grid cell formulation much influents the convergency and accuracy of computations.

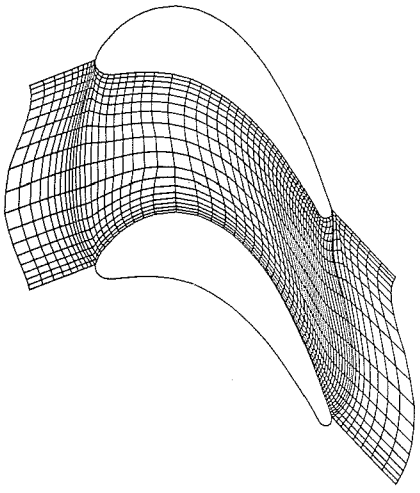

Fig.1. Principle scheme of generating x^1– coordinate lines

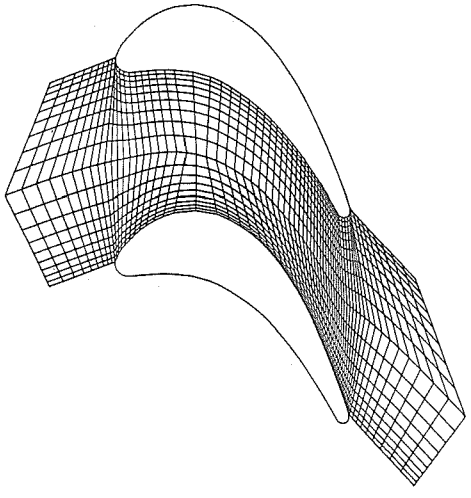

Fig.3. Grid system of a turbine cascade generated by ASSS method

In the present paper a noval method (ASSS method), based on analogy of staffs–springs system, for generating a body–fitted coordinate system is proposed. The body–fitted coordinate system generated by this method at the wall approximately keeps to be orthogonal. The first step is to obtain the geometrically central x^1–coordinate line. Then the x^1–coordinate lines are formed by proportion of the straight lines connecting the grids points of the central line with the corresponting grid points of both suction and pressure surfaces (see Fig.1). These x^1–coordinate lines are fixed in the later grid generation procedure. The third step is to generate the x^2–coordinate lines. On the one of the x^1–coordinate lines, for example the *j-th* x^1–coordinate line, the spacings between two grid points are replaced by springs. The effect of the approprite grid points at both walls on the position of the grid point of *j-th* x^1–coordinate line is similar to the effect of two bended staffs, the other ends of them are fixed at the pressure and section surfaces with the bending angles of α_{upp} and α_{low}, respectively. The following balance equation for each grid point we have

$$-C_{i-1}(S_i - S_{i-1}) + C_i(S_{i+1} - S_i)$$
$$+ M_{upp}\alpha_{upp}\varphi(J-j) - M_{low}\alpha_{low}\varphi(j-1) = 0 \qquad (19)$$

where: C_{i-1}, C_i denote the elasticity coefficients of the *i-th* and *(i+1)-th* springs, respectively. M_{upp}. and M_{low} denote moments of force from upper and lower walls, respectively. $\varphi(J-j)$and $\varphi(J-1)$are damping coefficients of upper grid point, *J*, and lower grid point, 1. Because the bending angles, $\alpha_{upp}, \alpha_{low}$, and position of S_i are related each to other, iterations for solving the above equations require greater CPU time consume. It can be simplified by the following approximation.

$$\alpha_{upp} = (S_{i\,upp} - S_i)/D_{upp}$$
$$\alpha_{low} = (S_i - S_{i\,low})/D_{low} \qquad (20)$$

where $S_{1\,upp}$ and $S_{i\,low}$ are the crosssection points between the *j-th* x^1-coordinate line and the normals to upper and lower walls, respectively. Then the Eq.(19) can be rewritten as:

$$-C_{i-1,j}S_{i-1,j} + \left[C_{i-1,j} + C_{i,j} + \frac{M_{upp}\varphi(J-j)}{D_{uppi,j}} + \frac{M_{low}\varphi(j-1)}{D_{lowi,j}}\right] S_{i,j} - C_{i,j}S_{i+1,j}$$
$$= \left[\frac{M_{upp}\varphi(J-j)}{D_{uppi,j}} S_{i,jup} + \frac{M_{low}\varphi(j-1)}{D_{lowi,j}} S_{i,jlow}\right] \qquad (21)$$

$(i = 2,...,I-1;\ j = 2,...,J-1)$

The coefficient $C_{i,j}$ is chosen to be an average value of $C_{i,j-1}$ and $C_{i,j+1}$ for smoothness of the coordinate lines generated, i.e.

$$C_{i,j} = \frac{1}{2}(C_{i,j-1} + C_{i,j+1})$$

or

$$-C_{i,j-1} + 2C_{i,j} - C_{i,j+1} = 0 \qquad (22)$$

The bonndary coditions at lower and uppar walls of above equation are

$$C_{i,J} = 1/(S_{i+1} - S_i)_1$$
$$C_{i,J} = 1/(S_{i+1} - S_i)_J \qquad (23)$$

respectively.

The values of $C_{i,j}$ are obtained by solution of Eq.(22).

Finally, The x^2–coordinate lines are obtained by solving Eq.(21). In this method iteration procedure is not required. The final grid system of a turbine blade cascade is shown in Fig.3. It is shown the the x^2–coordinate lines is closed to the normals.

Discretization and Solution

The integral equations, Eq.(1), can be discretized with summation around the four sides (numbered as l) of the rhombus cell and the variables are defined at the cell center, i.e.

$$\frac{d\rho}{dt} = -\frac{1}{V}\sum_{l=1}^{4}\rho_l(\vec{W}\cdot\vec{\Delta S})_l$$
$$\frac{d(\rho W_x)}{dt} = -\frac{1}{V}\left[\sum_{l=1}^{4}(\rho W_x)_l(\vec{W}\cdot\vec{\Delta S})_l + \sum_{l=1}^{4}(\hat{p}\Delta S_x)_l + \sum_{l=1}^{4}(\tau_x\Delta S)_l\right]$$
$$\frac{d(\rho W_y)}{dt} = -\frac{1}{V}\left[\sum_{l=1}^{4}(\rho W_y)_l(\vec{W}\cdot\vec{\Delta S})_l + \sum_{l=1}^{4}(\hat{p}\Delta S_y)_l + \sum_{l=1}^{4}(\tau_y\Delta S)_l\right] \qquad (24)$$

$$\frac{de}{dt} = -\frac{1}{V}\left[\sum_{l=1}^{4}(e+p)_l(\vec{W}\cdot\vec{\Delta S})_l + \sum_{l=1}^{4}(\vec{\tau}\cdot\vec{W})_l\Delta S_l\right]$$

where V is cell area, $\vec{\Delta S}_l = (\Delta S_{xl}, \Delta S_{yl})^T$ is the length vector of cell surface for twodimensional problem. W_x and W_y are the velocity components in x,y directions, respectively. $\vec{\tau} = (\tau_x, \tau_y)^T$ and $\hat{p}$ are viscous stress and pressure parameter, respectively. They will be discussed later.

Eq.(24) can be written in general form as:

$$\frac{d\Phi}{dt} + Q = 0 \qquad (25)$$

Since the variables are stored at the cell center, their values at cell surfaces are found by simple averaging of the quantities Φ from the adjacent cell centers. This kind of finite volume spatial discretization reduces to central difference scheme which is formally second order accurate for smooth grid. In order to suppress its well–known tendency for odd–even points decoupling, to capture shocks and to

minimize pre– and post–shock oscillation, an adaptive dissipation term D is added to the system, i.e.

$$\frac{d\Phi}{dt} + Q - D = 0 \tag{26}$$

The discretization equations, Eq.(25), are solved using the modified multi–stage Runge–Kutta time–marching method [15] . In the present paper the multigrid scheme is also applied to solve the algebraic equations. The auxiliary meshes are formed by doubling the mesh spacing and the informations of the flow variables are transfered to a coarser grid by the following principle:

$$\Phi_{2h}^{(0)} = \sum_{i=1}^{4} (V_{hi}\Phi_{hi} / V_{2h}) \tag{27}$$

where the subscripts denote the values of mesh spacing parameter. Then a forcing function is defined as:

$$P_{2h} = \sum_{i=1}^{4} (Q_h\Phi_h - D_h\Phi_h)_i - (Q_{2h}\Phi_{2h}^{(0)} - D_{2h}\Phi_{2h}^{(0)}) \tag{28}$$

The final equation, updating on a coarse grid, can be rewritten as

$$\frac{d\Phi}{dt} + Q - D + P = 0 \tag{29}$$

The process is repeated on successively coarser grids. Finally, then correction calcalated on each grid is passed back to the next finer grid by bilinear interpolations.

Results

Numerical solution method for transonic turbine and supersonic compressor cascades are presented and compared with experimental data. The computational grids are generated by the use of ASSS method.

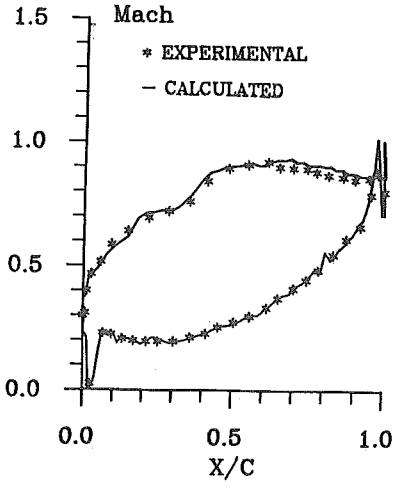

Fig.4. Mach number distributions on suction and pressure surfaces for the case of $M_{2is}=0.8$

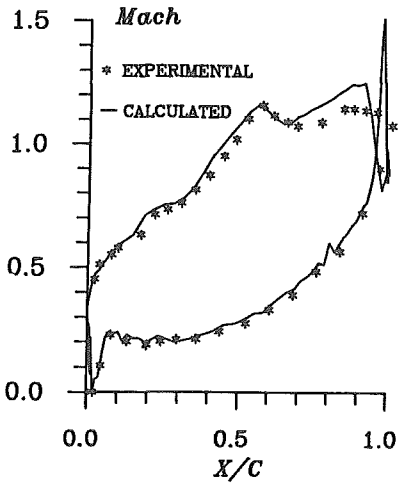

Fig.5. Mach number distribution on suction and pressure suffaces for the case of $M_{2is}=0.985$

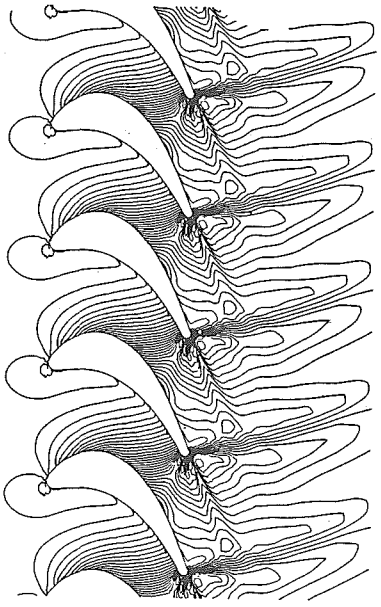

Fig.6. Density contour calculated (88 × 24)

VKI–LS59 turbine cascade [16]

The first example solution is for a transonic turbine cascade shown in Figs.3. This blade cascade was tested in four European wind tunnels [16] . Its relative pitch is 0.71, inlet flow angle is −30 ° . The inlet total temperture, total pressure and turbulence intensity are 290K, 103360 Pa and 1%, respectively. The outlet isentropic Mach number are about 0.8 and 0.985, respectively. The grid number is 124 × 32. The comparisons between the Mach number distributions on suction and pressure surfaces, calculated and tested, for isentropic outlet Mach numbers, 0.8 and 0.985, are

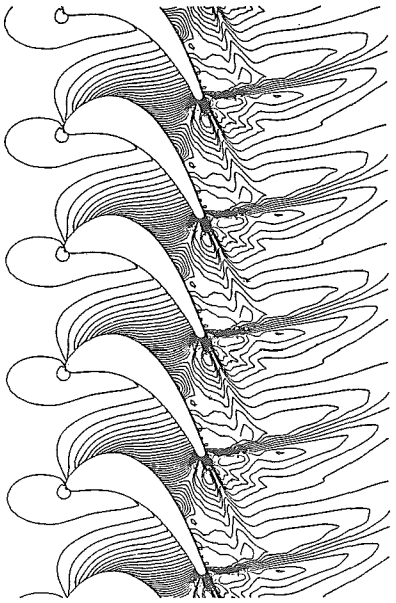

Fig.7. Density contour calculated (124 × 32)

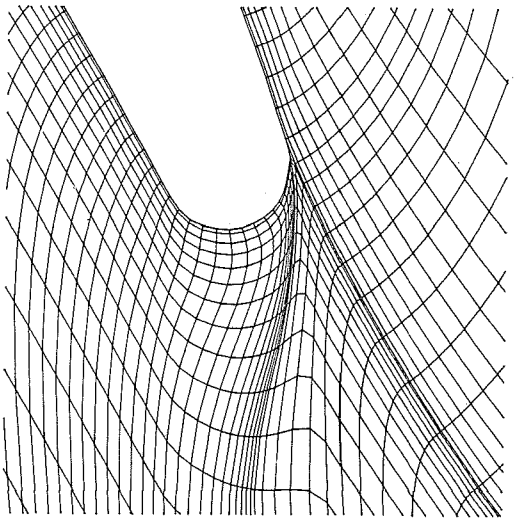

Fig.8. Coordinate system in the vicinity of trailing edge

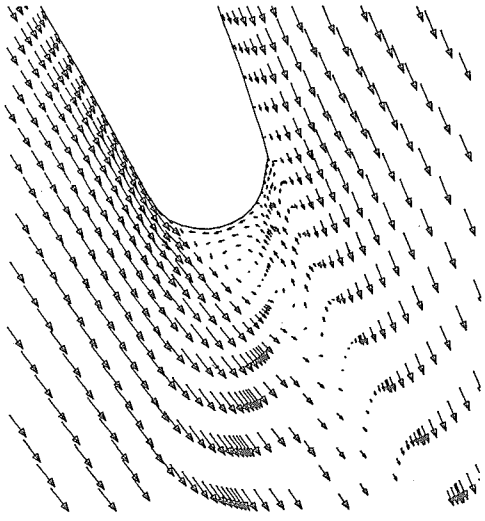

Fig.9. Vector scheme in the vicinity of trailing edge

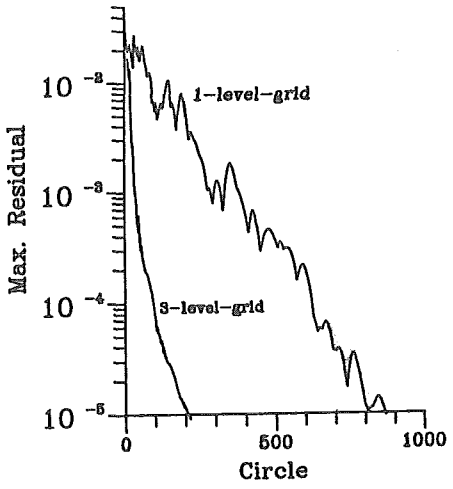

Fig.10. Convergence histories of multigrid scheme.

plotted in Fig.4 and Fig.5. The density contours of the Mach number of 0.85 for grid points 88 × 24 and 124 × 32 are shown in Fig.6 and Fig.7, respectively. The body–fitted coordinate lines in the vicinity of the trailing edge are shown in Fig.8. The velocity vector scheme in the same region as Fig.8 is plotted in Fig.9. It is seem that the flow deviates from the geometric outer angle. There is a pair of vortexes just behind the trailing adge. The large one is located on the left side and the small one on the right side. The convergence histories, shown in Fig.10, have shown the rapid convergence of using multigrid scheme.

Supersonic inlet flow compressor cascade

The socond example is a supersonic inlet flow compressor cascade tested in the supersonic compressor wind tunnel of the Institute of Engineering Thermophysics, Chinese Academy of Sciences. The inlet Mach number is 1.3. The inlet flow angle and blade stagger angles are 61.9 and 57.75 deg., respectively. The pressure ratio is 1.463 and the Reynolds number is 3.4×10^6. The grid system, shown in Fig.11, is also generated by the ASSS method. The grid number is 112 × 48 for both Euler equation and Navier–Stokes solutions, respectively. Fig.12 shows the

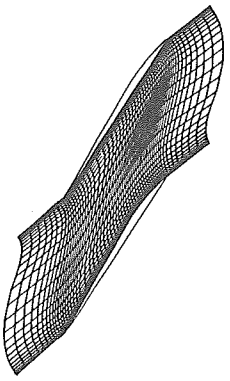

Fig.11. Grid system of compressor cascade

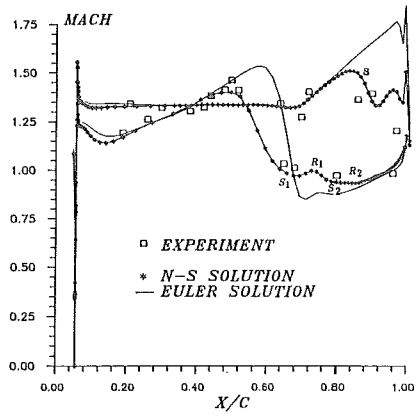

Fig.12. Calculated Mach number distributions on pressure and suction surfaces in comparison with experiment

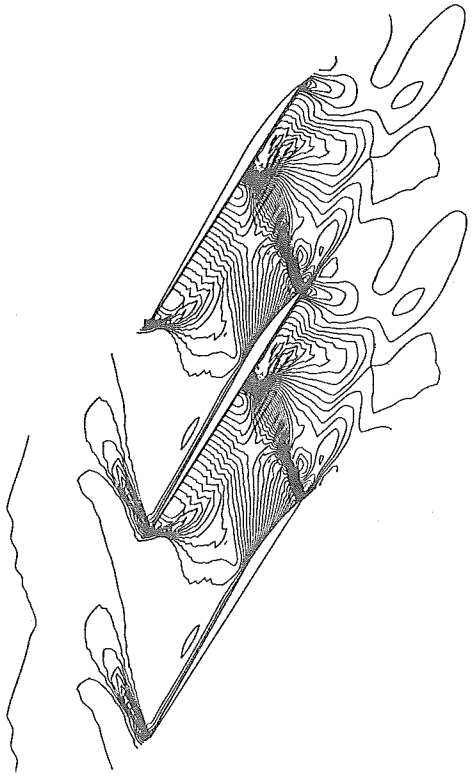

Fig.13. Density contour calculated by Euler solver

isentropic Mach number distributions of both solutions in comparison with experimental data. Figs. 13, 14 are the calculated density contours of both solutions. Fig.15 is a schlieren picture taken by Professors Yu Shen and Chen Jiagang of the Institute of Engineering Thermophysics. The mumerical solution of the Navier–Stokes solver agrees more better with the experiment than of the Euler solver. The shock of the Euler solver locates near trailing edge of suction surface and hits on pressure surface in a post–mid position. The calculated and the experimental results are looking fairly similar. As shown in Figs. 12, 14 and 15 the actual passage shock presents a λ–type shepe. Due to the shock wave separations are appeared on either side of the blade passage. Because of Shock–boundary layer interaction starting from point S of the suction surface the pressure have greatly increased (see. Fig. 12) and separation has occured (see. Fig. 16). Fig.12 apparently shows the picture of separation. On the pressure surface boundary layer has slightly separated from point S_1 and reattached at point R_1. At a distance from first reattachment pressure is increased again, then the slight separation and reattachment are reapeared. It can be found from the enlarged velocity vector scheme (Fig. 17).

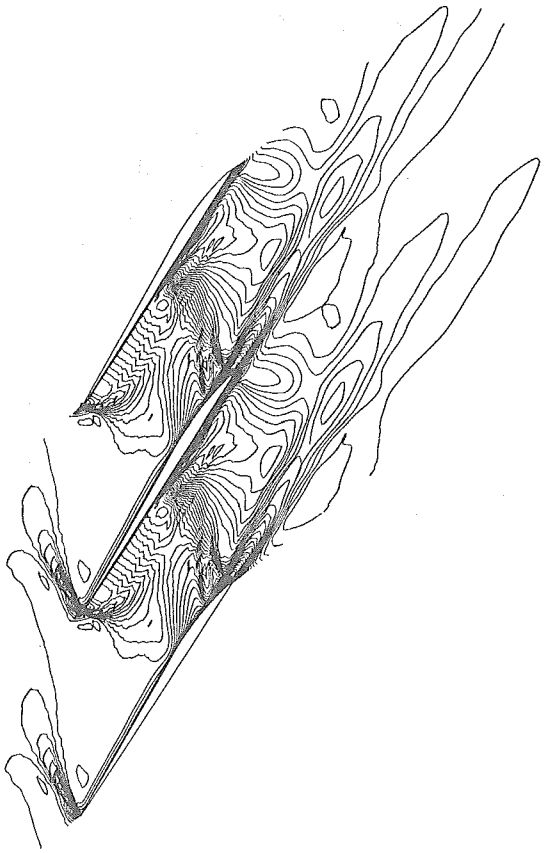

Fig.14. Density contour calculated by Navier–Stokes solver

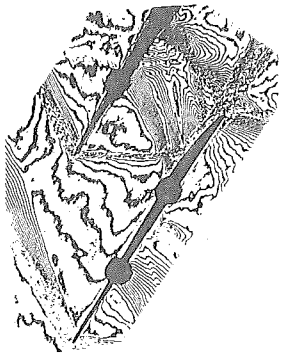

Fig.15. Schlieren picture of supersonic inlet flow compressor cascade

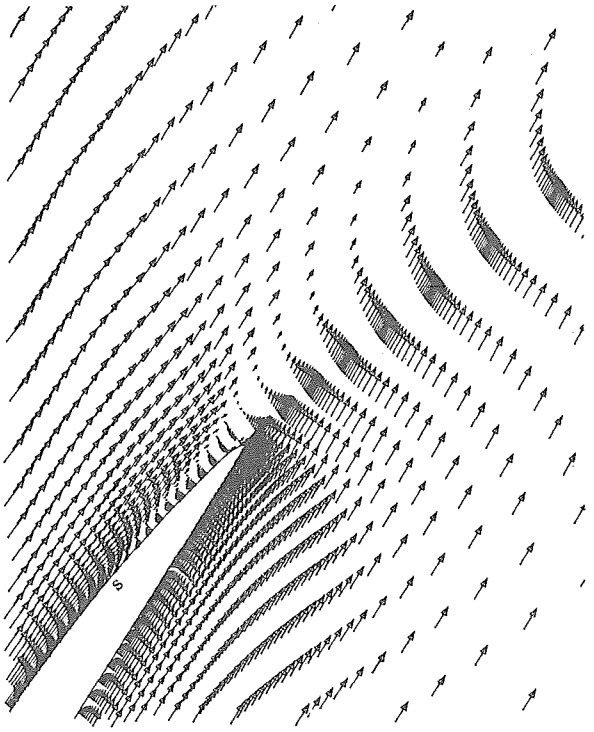

Fig.16. Velocity vector scheme in the region of the rear portion of blade

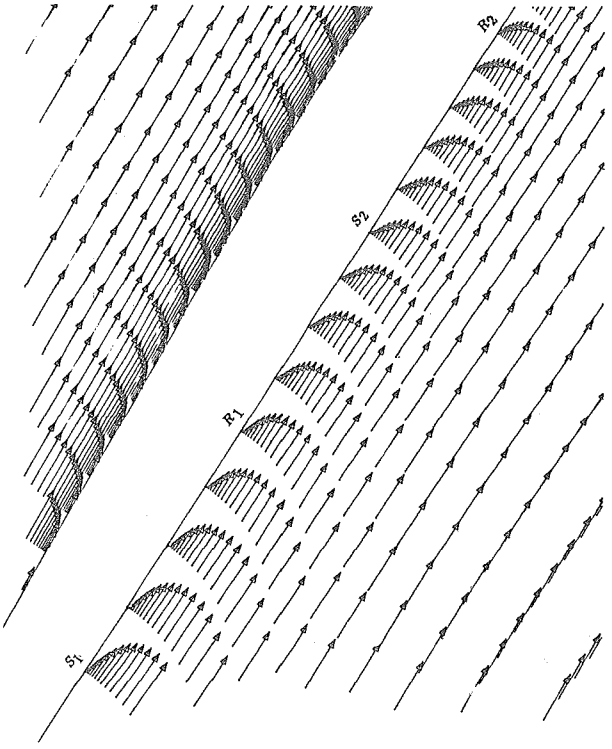

Fig.17. Velocity vector scheme in the rigion of boundary layer separaions and reattachments on the pressure surface.

Conclusions

A time–marching explicit finite volume method with multigrid scheme has been presented for solving both Euler and Navier–Stokes equations with application to steady two–dimensional transonic flows in turbomachinery cascades. A new method expressing viscous terms of the Navier–Stokes equations has been also proposed. The method is more simple in comparison with previous methods. Based on analog of staffs–springs system a rapid grid generation technique of a body–fitted coordinate system with approximately normal coordinate lines to the walls has been suggested. The discretized algebraic equations with multigrid scheme are solved by Runge–Kutta method.

Numerical solution results for two turbomachinery cascades have been presented and compared with experimental data to demonstrate the accuracy and computational efficiency of the analysis method. The method has good capability of capturing shock waves.

For simplicity, the presentation of the numerical method was applied to planar, two–dimensional cascade flows. The method, however, can be applied to three–dimensional turbomachinery flows.

References

〔1〕 Lax, P.D. and Wendrott, B., "Difference Schemes for Hyperbolic Equations with High Order Accuracy," Comm. Pure. App. Math., 17, pp.381–398, 1964.

〔2〕 McDonald, P.W. et al., "The Computation of Transonic Flow Through Two Dimensional Gas Turbine Cascades", ASME Paper 71–GT–89, 1971.

〔3〕 Maccormack, R.W. and Baldwin, B.b., "A Numerical Method for Solving the Navier–Stokes Equations with Application to Shock–Boundary Layer Interactions," AIAA Paper 75–1, 1975.

〔4〕 Denton, J.D., "A Time Marching method for Two– and Three–Dimensimal Blade–to–Blade Flow," ARC R and M 3775, 1975.

〔5〕 Jameson, A. and Turkel, E., "Implicit Schemes and the LU Decompositions," Mathematics and computation, Vol.37, pp.385–390, 1981.

〔6〕 Jameson, A., Schmidt, W. and Turkel, E., "Numerical Solutions of the Euler Equations by Finite Volume Methods Using Runge–Kutta Time Stepping Schemes," AIAA Paper 81–1259, 1981.

〔7〕 McDonald, P.W. et al., "A Comparison Between Measured and Computed Flow Fields in a Transonic Compressor Rotor", ASME Journal of Engineering for Power, Vol. 104, 1981.

〔8〕 Denton, J.D. et al., "An Improved Time–Marching Method for Turbomachinery Flow Calculation," ASME Paper 82–GT–239, 1982.

〔9〕 Ni, R.H., "A Multiple Grid Scheme for Solving

the Euler Equations", AIAA Journal, Vol.20, NO.11, pp.1565–1571, 1982.
〔10〕 Dawes, W.N., "A Numerical Analysis of Viscous Flow in a Transonic Compressor Rotor and Comparison with Experiment," ASME Journal of Engineering for Gas Turbine and Power, Vol. 109, No.1, pp.83, 1987.
〔11〕 Briley, W.R. and McDonald, H., "Solution of the Multidimensional Compressible Navier–Stokes Equations by a Generalized Implicit Method", Journal of Computational Physics, Vol.24, pp.372, 1976.
〔12〕 Beam, R.M. and Warning, R.F., "An Implicit Factored Scheme for the Compressible Navier–Stokes Equations," AIAA Journal, Vol.16, No.4, 1978.
〔13〕 Shamroth, S.J., McDonald, H. and Briley, W. R., "Application of Navier–Stokes Analysis to Transonic Cascade Flow Fields," ASME Journal of Engineering for Power, 1982.
〔14〕 Baldwin, B. and Lomax, H., "Thin Layer Approximatoin and Algebraic model for Separated Turbulent Flows," AIAA Paper 78–257, 1978.
〔15〕 Zheng Xiaoqing, Xu Yanji and Chen Naixing, "Aerodynamic Calculation of Turbomachine Cascade Flows with Shocks Using Euler and Navier–Stokes Solvers," Paper presented at the Asian Pacific Conference on Computaional Mechanics held in Hong Kong, 11–13 December,1991.
〔16〕 Kiock, R. et al., "The Transonic Flow through a Plane Turbine Cascade as Measured in Four European Wind Tunnels," ASME 85–IGT–44, 1985.